Sequential Crystallization Kinetics of Poly(*p*-phenylene sulfide) Doped with Carbon or Graphite Particles

JEN-M. CHEN and E. M. WOO*

Department of Chemical Engineering, National Cheng Kung University, Tainan, Taiwan, 701-01, Republic of China

SYNOPSIS

Isothermal crystallization kinetics were investigated by differential scanning calorimetry (DSC) for poly(*p*-phenylene sulfide) (PPS) doped with amorphous carbon or crystalline graphite particles. Both types of carbon forms have been found to affect the crystallization behavior of PPS to different extents. The crystalline graphite particles have a more pronounced effect on the overall rate as well as mechanisms of PPS crystallization than do the amorphous carbon particles. Relative contributions and competition from crystallizations of two different crystals in the later-stage crystallization of PPS have been found to cause the phenomenon of deviation from linearity in the Avrami plots. A sequential crystallization model has been shown to describe well the crystallization behavior of the PPS doped with the particles. © 1995 John Wiley & Sons, Inc.

INTRODUCTION

Crystallization is one of the most studied subjects in polymer physics. The crystallization of filled or reinforced polymers can also be influenced by factors including fillers, fibers, additives, or temperature. Poly(phenylene sulfide) (PPS) is a high-temperature semicrystalline thermoplastic polymer with many desirable mechanical properties. PPS is finding versatile uses in technological applications such as electronic component encapsulants, conducting polymers, printed circuit boards, and optical fibers.[1,2] More recently, PPS has also been considered for use as a matrix material in fiber-reinforced composites. PPS has a strong tendency to crystallize when cooled to temperatures below its melting temperature (270–290°C). Its properties, therefore, are greatly influenced by the kinetic process of the crystallization and, consequently, by the morphological microstructure developed during processing. There have been a large number of studies[3–10] dealing with the crystallization behavior of neat or reinforced PPS in the past few years. It has become well known that the degree of crystallinity and/or morphology can be influenced directly by the thermal treatment during processing and that the thermal treatment subsequently influences the mechanical properties of the processed polymers. Desio and Rebenfeld[4,5] and Auer et al.[6] studied the effects of various reinforcing fibers on the crystallization rate of PPS and found that the fiber types (carbon, aramid, or glass) as well as the fiber sizings may affect the crystallization rates. They found that both carbon and aramid fibers caused a decrease in the crystallization half-times, with the aramid fiber exhibiting a more pronounced effect and the glass fiber having almost no effect at all.

The crystallinity–property and morphology–property relationships of neat PPS and fiber composites have also been well studied.[11,12] Transcrystalline growth of PPS on the interface of reinforcing fibers has been one of the most studied subjects. Nucleating effects of fibers have been reported by Zeng and Ho,[13] who observed that single-carbon and glass-fiber filaments embedded in a thin film of PPS resin exhibited a pronounced nucleating effect. However, the reported effects of fibers on the total crystallinity of PPS seemed inconsistent among various researchers. Some concluded a higher degree of crystallinity of carbon and glass-reinforced PPS,[14,15] while others reported a decrease in crystallinity.[16] Correlation between the transcrystalline

* To whom correspondence should be addressed.

Journal of Applied Polymer Science, Vol. 57, 877–886 (1995)
 CCC 0021-8995/95/070877-10

crystals and effects on crystallization kinetics have yet to be investigated.

While the commercial carbon/graphite reinforcing fibers offer a unique aspect of studies on understanding the effect of reinforcing materials on PPS crystallization, they, however, may introduce complicating factors such as different degrees of surface treatment, various levels of graphitization, or effects of sizings, which all can affect crystallization mechanisms and kinetics. To simplify the observation, we investigated the kinetics of crystallization of PPS doped with carbon or graphite particles instead of complicated fiber systems in this study.

EXPERIMENTAL

Materials and Preparation

Two types of carbon filler were used: amorphous carbon black and crystalline graphite particles. The carbon or graphite particles have an average size of about 70–90 μm. Poly(phenylene sulfide) (PPS) was obtained from commercial sources (Philips Petroleum Co., Ryton V-1) in fine powder form—melt viscosity = 90 Pa-s, and M_n = 15,000 g/mol. The PPS was compounded with micron-sized carbon or crystalline graphite particles with the solid loadings ranging from 5 to 50 wt %. Compounding of the solid fillers with PPS was performed by direct melt blending or solvent mixing. The solvent mixing was done by dissolving the PPS in α-chloronaphthalene (Merck Co.) at 210°C under continuous stirring with the solid particles being added gradually. After solvent mixing, the compounded PPS–filler mixture was placed in a vacuum oven at 200°C until all the residual solvent was completely evaporated.

Differential Scanning Calorimetry

Differential scanning calorimetry (DSC) offers a convenient, accurate method of following quantitatively the crystallization progress and analysis of crystallization parameters. The crystallization kinetics of PPS were investigated by observing the heat flow from an isothermal DSC scan as a function of time. A power-compensated type of differential scanning calorimeter (Perkin-Elmer DSC-7, equipped with an intracooler and a DEC computer for data acquisition/analysis) was used for various thermal treatments of the samples and to observe the melting endotherm peaks. Prior to DSC runs, the temperature and heats of reaction were calibrated with indium and zinc standards. Relatively small sample sizes (4–7 mg) were used to minimize the heat-transfer effect of low thermal conductivity of the polymer. The sample was heated in the DSC quickly to 320°C, held there for 5 min to eliminate residual crystals, then quenched (at −320°C/min) to the designated crystallization temperature, and data acquisition was begun immediately. For bringing the samples to the crystallization temperature from the pretreatment temperature above the melt, the fastest cooling rate (−320°C/min) was necessary to prevent any effect of nonisothermal crystallization, during the ramping transient, on the magnitudes of heat to be measured. During the pretreatment, isothermal crystallization, or DSC scanning, a nitrogen purge was provided throughout the run. The isothermal melt-crystallization experiments were performed at four to five different temperatures between 220 and 250°C. For experiments on the melting behavior of primary and minor crystals, a uniform heating rate of 10°C/min was used.

RESULTS AND DISCUSSION

Carbon Black and Graphite Particulate Fillers in PPS

Crystallization isotherms for the carbon- or graphite-filled PPS samples were generated at five isothermal temperatures: 220, 230, 240, 245, and 250°C. For the kinetic analysis of the filled PPS samples, the well-known Avrami equation[17,18] was employed for preliminary analysis:

$$1 - X_t = \exp[-kt^n] \qquad (1)$$

where X_t is the relative crystallinity at time t; k, the crystallization rate constant depending on nucleation and growth rates; and n, the Avrami crystallization exponent depending on the nature of nucleation and growth geometry of the crystals. Avrami plots were constructed from these isotherms by plotting $\log[-\ln(1 - X_t)]$ vs $\log(t)$ for the carbon-filled PPS samples (5–50 wt % of carbon) and the graphite-filled PPS samples (5–50 wt % of graphite).

Effect of Fillers on Crystallization Exponent

To examine the effects of the carbon or graphite fillers on the mechanisms and rates of crystallization of PPS, Avrami plots were similarly constructed. Figures 1 and 2 show that the Avrami plots for the two amorphous carbon-filled PPS samples (5 and 10 wt %, respectively) are mostly linear straight

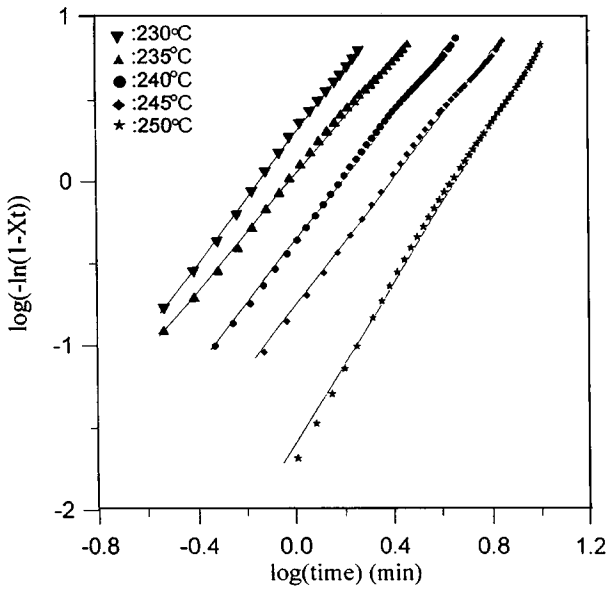

Figure 1 Avrami plots of carbon (5 wt %)-filled PPS samples crystallized at 230, 235, 240, 245, and 250°C.

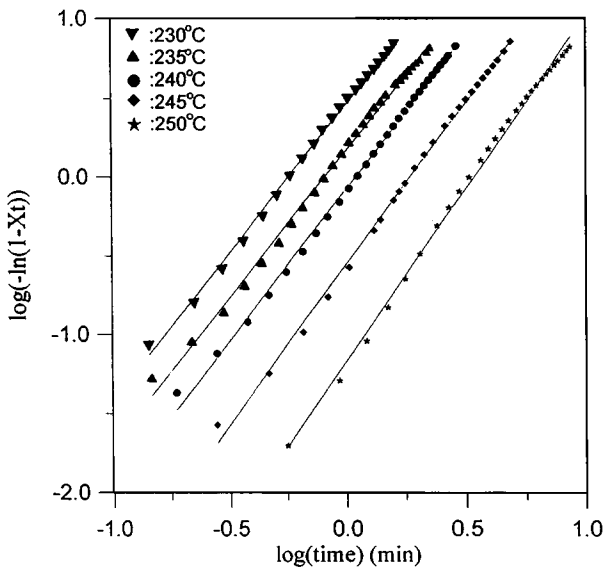

Figure 2 Avrami plots of carbon (10 wt %)-filled PPS samples crystallized at 230, 235, 240, 245, and 250°C.

lines. Only at a few isothermal crystallization temperatures did the plots exhibit barely visible deviation from linearity at a later stage of crystallization (i.e., at relative crystallinity $X_t > 0.98$). The carbon-filled PPS samples of other filler contents (from 10 to 50 wt %) were found to behave similarly to the one with 5 or 10 wt % of carbon. The kinetic constants derived from the plots for all carbon-filled PPS are listed in Table I. The exponents derived from the slopes of the plots for the carbon-filled PPS, however, were lower than those reported for the neat PPS from our previous study.[19] The exponents for the carbon-filled PPS were found to be 1.7–1.9, while the exponents for neat PPS are 2.2–2.5. The values of n for the carbon-filled PPS are lower by 0.5–1.0 in comparison with the neat PPS, suggesting that the nucleation mechanism might have changed from homogeneous to heterogeneous.[20] Clearly, the fillers have altered the mechanism of PPS crystallization. The lower exponent for the carbon-filled PPS suggests a change of the crystal growth mechanism at the later stage of crystallization.

Interestingly, the crystallization behavior of the graphite-filled PPS was found to be significantly different from that of the carbon-filled PPS. In contrast with the almost linear Avrami plots of the carbon-filled PPS, an easily identified discontinuity was observed in the Avrami plots for the graphite-filled PPS at the later stage of crystallization ($X_t = 0.9$), at which the slope (the exponent n) decreases. Figures 3 and 4 show that the Avrami plots for the graphite-filled (10 and 25 wt %) PPS sample are no longer straight lines but yield two segments with distinctly different values of n corresponding to each of the two linear portions. Similarly, plots of the graphite-filled PPS samples of other filler contents were also found to exhibit a discontinuity. The kinetic constants derived from the plots for the graphite-filled PPS samples crystallized at all isothermal temperatures are listed in Table II. Two apparent Avrami exponents (n_1 and n_2) for the graphite-filled PPS were determined from the slope of the plots. The values of the exponents n_1 determined from the first linear segment were 1.7–2.0, which are about the same as the values of exponents

Table I Effect of Carbon Contents on Crystallization Kinetics of Carbon-filled PPS

Carbon in PPS (Wt %)	T_c (°C)	n_1	k_1 (min^{-n_1})	$t_{1/2}$ (min)
5	230	1.8	2.02	0.56
5	235	1.8	1.15	0.76
5	240	1.8	0.57	1.11
5	245	1.8	0.21	1.93
10	230	1.7	2.05	0.53
10	235	1.8	1.22	0.73
10	240	1.9	0.57	1.11
10	245	1.9	0.21	1.89
25	230	1.7	2.0	0.53
25	235	1.6	1.25	0.69
25	240	1.6	1.25	0.99
25	245	1.7	0.25	1.83

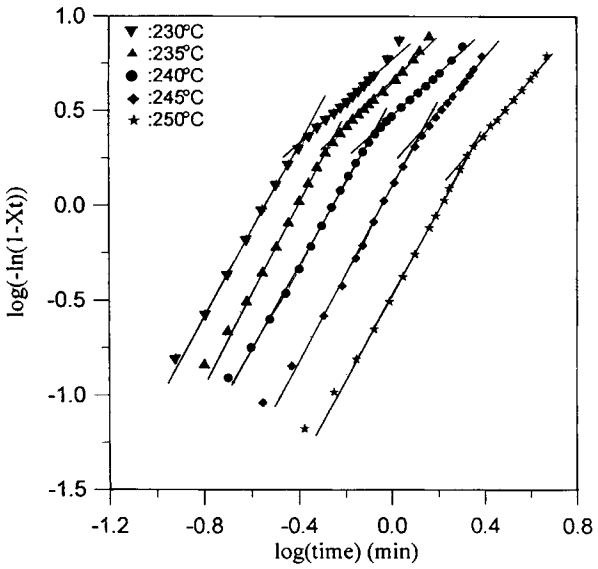

Figure 3 Avrami plots of graphite (10 wt %)-filled PPS samples crystallized at 230, 235, 240, 245, and 250°C.

obtained for the carbon-filled PPS. The carbon-filled PPS system, however, does not exhibit a discontinuity in the Avrami plots. The values of n_2 determined from the second linear segment of the plots for the graphite-filled PPS were 1.1–1.6. The widely differing values of n_1 and n_2 suggest that there obviously were two different mechanisms that evolved at different stages of the crystallization for the graphite-filled PPS, which will be further discussed in terms of series-parallel growth of primary and secondary crystals in later sections of this report.

Effect of Fillers on Crystallization Half-times

To understand how the overall crystallization rate was affected by the fillers, the crystallization half-times were compared for neat PPS, PPS/carbon, and PPS/graphite systems. The crystallization half-time is defined as the time at which the crystallization is half (50%) completed. A shorter half-time reflects a faster crystallization rate and vice versa. Figure 5 shows the half-time of crystallization ($t_{1/2}$) plotted as a function of isothermal crystallization temperature (T_c) for the neat PPS, PPS samples filled with carbon black (at 5 wt %), and PPS/graphite particles samples (at 5 wt %), respectively. The crystallization half-times were found to decrease significantly for the two filled PPS systems, indicating a marked effect of the filler on enhancing the overall crystallization rate. While the two types of filler particles both enhanced the crystallization rate, the graphite particles, by comparison, had a more pronounced effect than did the amorphous carbon black on enhancing the crystallization rate of PPS. Apparently, the type of fillers (carbon vs. graphite) influenced the rate as well as the mechanisms to different extents.

The same enhancement effect was also observed for the carbon- or graphite-filled PPS samples of other contents (10–50 wt %). The rate increase, however, did not increase with the filler content in PPS. The crystallization half-time plotted as a function of the filler contents is shown in Figure 6. Graphite particles more effectively increase the crystallization rate. However, an increase in the filler contents does not seem to have any effect in the range of filler contents investigated (5–50 wt %). Our interpretation for the change in the crystallization kinetics is that the nucleation capability of the filler particles may be dependent on the crystal structure of the particle surface with which PPS interacts. Noncrystalline surfaces, such as amorphous carbon, are less able to provide sites for initiating nucleation than, e.g., are the crystalline graphite particles.

Solvent Effect on Doped PPS

It was also found during the course of this study that the behavior of the solvent-compounded PPS/filler mixtures was completely different from the melt-processed counterparts. One of our reports on similarly related studies has attempted to demonstrate the effects of solvent treatment of neat PPS

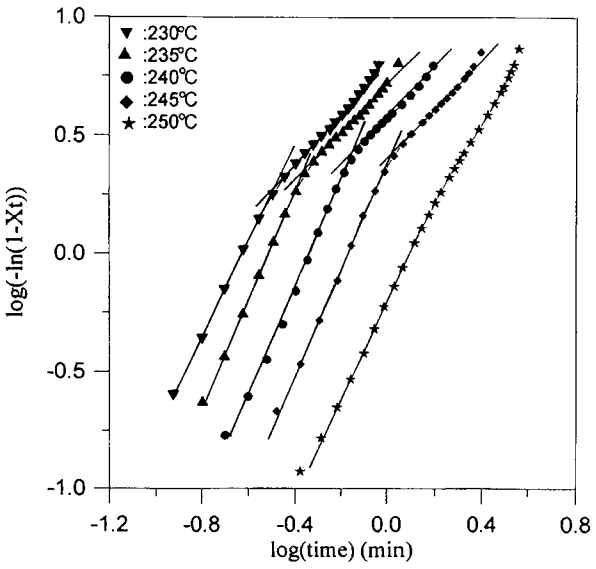

Figure 4 Avrami plots of graphite (25 wt %)-filled PPS samples crystallized at 230, 235, 240, 245, and 250°C.

Table II Effect of Graphite Contents on Crystallization Kinetics of PPS

Graphite in PPS (Wt %)	T_c (°C)	n_1	k_1 ($\min^{-n_1}$)	n_2	k_2 ($\min^{-n_2}$)
5	230	1.8	8.5	1.3	5.5
5	235	1.9	3.8	1.4	3.6
5	240	1.9	2.0	1.3	2.1
5	245	2.0	0.9	1.3	1.4
10	230	2.0	12.3	1.2	6.3
10	235	1.9	5.4	1.3	4.6
10	240	1.9	2.8	1.3	2.8
10	245	1.9	1.0	1.7	1.3
25	230	1.7	11.5	1.1	6.5
25	235	1.7	7.4	1.1	5.2
25	240	1.7	3.1	1.1	3.7
25	245	1.6	1.7	1.1	2.4

on the crystallization kinetics.[19] Solvent compounding induced higher melt crystals that were more difficult to destroy at the precrystallization melting treatment at 320°C. Residual crystals left in the crystallizing PPS may provide extra solvent-induced nucleation sites in addition to the nucleation sites provided by the solid filler particles. Additionally, it has also been suggested that the increased nucleation could be due to occluded α-chloronaphthalene solvent in the dried PPS sample.

The solvent-compounded mixtures of PPS with carbon black or graphite powders were similarly analyzed for understanding the crystallization kinetics. Figure 7 shows the Avrami plots for the solvent-processed carbon (5 wt %)–PPS samples. The plots are no longer straight lines, indicating that solvent compounding obviously introduced additional effects on the crystallization behavior of the carbon- or graphite-filled PPS. The kinetic constants derived for the solvent processed carbon- or graphite-filled PPS samples are listed in Table III. Solvent compounding of the filled PPS is seen to further increase the crystallization rates.

The carbon-filled PPS system did not exhibit a discontinuity in the Avrami plots. However, the sol-

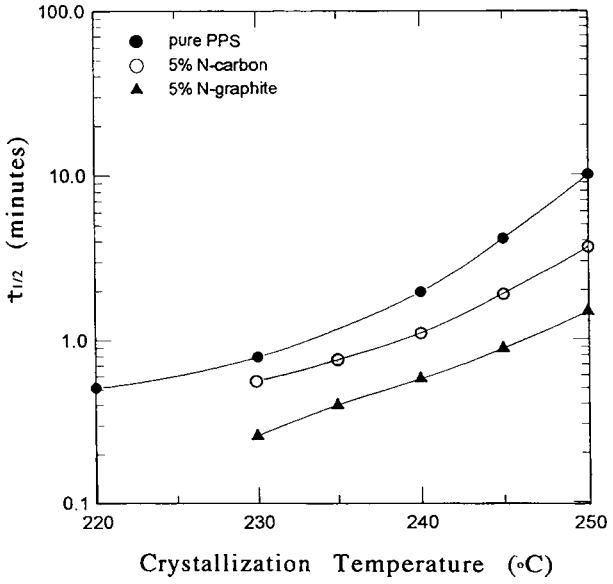

Figure 5 Comparison of crystallization half-times ($t_{1/2}$) for neat PPS and PPS doped with carbon or graphite particles at various temperatures.

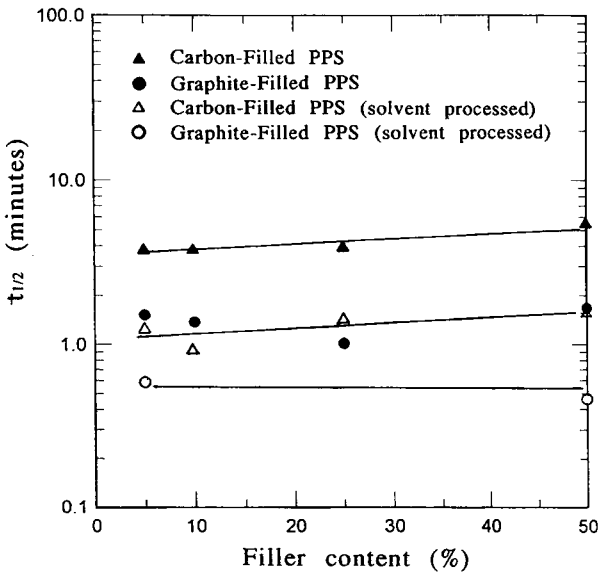

Figure 6 Crystallization half-times as a function of filler contents for the carbon- and graphite-filled PPS samples.

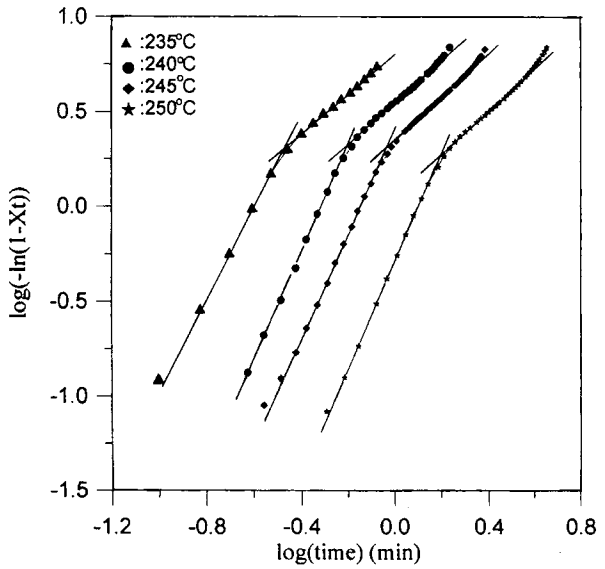

Figure 7 Avrami crystallization plots of solvent-processed PPS doped with carbon (5 wt %) at four isothermal temperatures.

vent-processed carbon–PPS samples exhibited a discontinuity in the Avrami plots and different values of the exponents. The graphite-filled PPS systems, processed with or without the solvent, both yielded nonlinear Avrami plots. The crystallization mechanisms were obviously affected to different extents by the presence of different types of fillers. Additionally, the solvent processing might have introduced additional factors.

It seemed interesting that the phenomenon of slope changes was observed in the graphite-filled PPS, but not observed in the carbon-filled PPS or the virgin neat PPS. The melting behavior of PPS[21–23] and poly(ether ether ketone) (PEEK)[24,25] have been found to exhibit multiple melting peaks when crystallized at more than two temperatures and held for a sufficient time. Although multiple melting behavior involving more than one minor melting peak below the regular major peak in polymers has been reported by many, there has not been any direct evidence showing a relationship between the minor melting peak and the observed crystallization results. Generally, the higher-temperature crystal entity is quite well established before the lower-temperature crystal entities form during the crystallization process. While there are several studies suggesting that the higher-temperature crystals are a result of remelting/recrystallization of the lower-temperature crystals,[26] there are other reports[27–29] pointing out that each of the entities evolves independently and coexists in the so-called dual morphological structure. Polymorphism or a morphology with more than one unit cell has also been reported for cold-crystallized,

Table III Effect of Carbon Contents on Crystallization Kinetics of PPS (Samples Processed with α-Chloronaphthalene Solvent)

Filler Contents (Wt %)	T_c (°C)	n_1	k_1 ($\min^{-n_1}$)	n_2	k_2 ($\min^{-n_2}$)
Carbon–PPS					
5	235	2.3	22.39	1.1	6.3
5	240	2.3	5.2	1.1	3.47
5	245	2.2	1.86	1.3	2.1
5	250	2.5	0.5	1.2	1.0
10	235	2.3	24.5	1.2	7.59
10	240	2.5	7.6	1.5	4.47
10	245	2.4	2.7	1.6	2.75
10	250	2.3	0.76	1.7	1.15
25	240	1.4	1.8	1.0	1.4
25	245	1.5	1.1	1.1	0.9
25	250	1.6	0.43	1.1	0.42
Graphite–PPS					
5	230	2.8	75.9	1.0	6.0
5	235	3.5	54.9	1.4	6.0
5	240	3.4	19.5	1.3	4.2
5	245	3.2	5.4	1.1	2.5
25	240	2.0	5.7	1.1	4.2
25	245	2.0	1.9	1.6	2.2

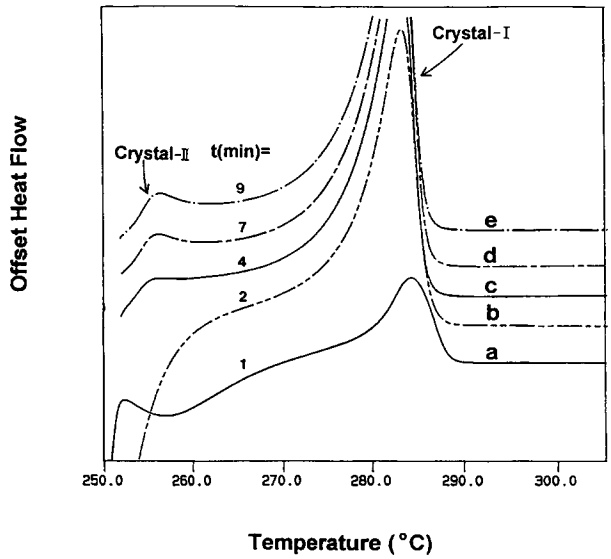

Figure 8 DSC endotherms showing the sequence of appearance of the multiple melting peaks as functions of crystallization time for the carbon-doped PPS samples.

melt-crystallized, or solvent-crystallized samples of poly(aryl ether ketone).[30-32]

DSC Evidence of Sequential Growth of Two Crystal Types

Earlier, Budgell and Day[7] attempted to explain the phenomenon of discontinuous Avrami plots for PPS and some other polymers by assuming that the two portions of the curves were due to crystallization of two types of crystals formed at different times of crystallization. However, they provided no direct evidence. Cebe and Chung[21] also proposed a preliminary correlation between the formation of primary and secondary crystals by observing the melting behavior for PPS. In this study, we attempted to provide more convincing evidence for the mechanism of sequential development of two different types of crystal entities by conducting DSC melting studies on PPS samples crystallized for various times before a model was proposed to explain the observed crystallization behavior.

Figure 8 shows the DSC melting endotherms (curves a–e) of the dual peaks of the carbon-filled PPS samples that had been subjected to various periods of crystallization time at 250°C. A minor, low-temperature peak is observed in the DSC thermograms (curves c–e) of the samples that had been crystallized for 4 min or longer. On the other hand, for the samples crystallized for times less than 4 min, the low-temperature peak is not observed (curves a and b). As the crystallization time is increased, the low-temperature peak is seen to increase in magnitude as well as in the peak temperature location. A quantity, α, is defined as

$$\alpha = (\Delta H_2)/(\Delta H_1 - \Delta H_{1,ti}) = (\Delta H_2)/\Delta(\Delta H_1) \quad (2)$$

where ΔH_1 is the final melting enthalpy related to the high-temperature crystal (Crystal-I), and $\Delta H_{1,ti}$, the melting enthalpy for the high-temperature crystal (Crystal-I) when the low-temperature crystal is just initiated at time t_i. The difference of these two terms $(\Delta H_1 - \Delta H_{1,ti})$ is the enthalpy increase of the Crystal-I from t_i to final time. ΔH_2 is the final melting enthalpy of the low-temperature crystal (Crystal-II). The ratio α therefore indicates relative contributions of the low-temperature and high-temperature crystals in the later-stage crystallization, which occurs after t_i. A greater contribution from the low-temperature crystal could result in a deviation from the original crystal growth from the high-temperature crystal. If this is the cause of the observed nonlinearity phenomenon in the Avrami crystallization plots, the t_i observed in the DSC melting peak results should be the same as the time (t_d) at which the discontinuity is located in the Avrami plot. Table IV lists the results of these quantities generated from the DSC observations. The t_i and t_d for various PPS systems are also compared in the same table. Since

Table IV Ratios of Melting Enthalpy Changes of Low-Melt vs. High-Melt Crystals after t_i or t_d

Samples	t_i (min)	t_d (min)	α
Virgin neat PPS	4	None	0.11
Carbon (10%)–PPS	3	None	0.13
Solvent-processed samples[a]			
Neat PPS[a]	3	2.5	0.56
Carbon (5%)–PPS[a]	2	1.6	0.53
Graphite (5%)–PPS[a]	1	0.7	1.67

[a] PPS doping with particles was done by α-chloronaphthalene solvent.

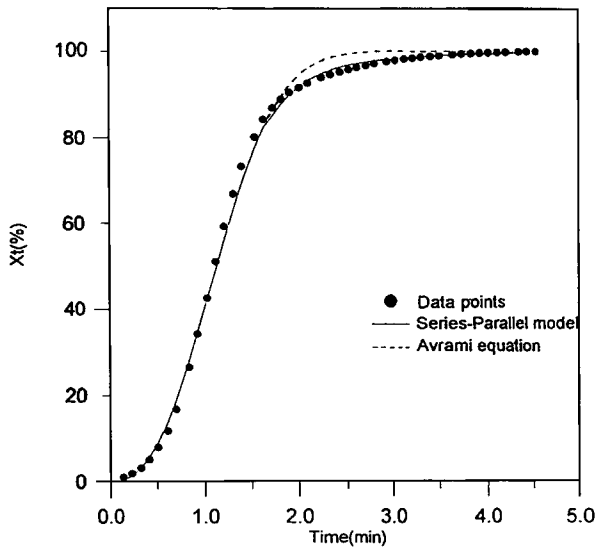

Figure 9 Series-parallel model fitting with the 250°C crystallization data of the carbon-doped PPS samples processed with solvent.

the samples for DSC melting experiments were crystallized for different times in 1 min increments, the reported t_i values would have an approximate error of ±0.5 min. Within acceptable experimental errors, these two observed times are seen to agree quite well. Obviously, the systems that exhibited two portions of the Avrami plots all have a greater value of α, indicating a greater contribution from the growth of the minor crystal. These observations should provide direct evidence for the mechanism of sequential appearance of the primary and minor peaks in the DSC melting endotherms of the PPS samples subjected to various crystallization times, suggesting that the primary and secondary crystal entities might evolve in series during the later stage of crystallization.

Model for Sequential-Parallel Growth of Two Crystals

The Avrami eq. (1) was found to be adequate for describing the crystallization behavior of the carbon-filled PPS or the neat PPS since the Avrami plots for these two PPS systems were all straight lines with no apparent discontinuity. However, when applied to describe the PPS systems showing relatively more significant growth of the low-temperature crystals in the later stage of crystallization, the Avrami equation [eq. (1)] was found to deviate pronouncedly. A parallel crystallization model was proposed earlier by Velisaris and Seferis[33] for describing the nonlinear behavior of the Avrami plots of PEEK. In their model, the kinetic constants were generated by curve fitting. As a result, some of the fitting parameters were difficult to be correlated to realistic physical significance. A later modification and improvement has been done by Cebe.[34] However, the parallel model by Velisaris and Seferis or the later modification by Cebe was based on a parallel assumption of the primary and secondary crystallization. Direct experimental evidence supporting the assumed parallel crystal growth, though, was not given in those studies.

To describe the crystallization of the primary crystal growing initially followed by sequential growth of the secondary crystal at $t = t_d$ in parallel with the still growing primary crystal, the result is expressed by the following two equations, each describing one of the two stages:

First-stage crystallization occurring at $t < t_d$,

$$X_{t1} = 1 - \exp[-k_1 t^{n_1}] \quad (3A)$$

Second-stage crystallization occurring at $t > t_d$,

$$X_t = X_{t1} + \omega_I[1 - \exp(-k_1 t^{n_1})] + \omega_{II}[1 - \exp(-k_2'(t - t_d)n_2')] \quad (3B)$$

where the constants bear the same symbol meanings as those in eq. (1), except that the subscript "1" refers to the first stage and "2" refers to the later (second) stage of crystallization. In the equation, ω_I and ω_{II} are the weight factors representing the quantities of the high-temperature and low-temperature crystals, respectively, developed in the second stage. Earlier, the DSC results on the melting behavior of the primary and secondary crystals of PPS demonstrated the fact of sequential appearance of two melting peaks, suggesting that the crystal entities appeared sequentially. The growth in the second stage of crystallization can be described by a parallel expression following the preceding growth of the major crystal. The overall crystallization could therefore be expected to be more reasonably described by a series-parallel expression, as represented by eqs. (3A) and (3B).

Figure 9 shows that the series-parallel crystallization model (solid line) describes well the crystallization behavior of the carbon-filled PPS (processed with solvent) at 250°C. The prediction by the unmodified Avrami equation (dashed line) shows significant deviation in the later stage of crystallization. Since the first-stage crystallization was entirely populated by the primary crystal, the kinetic constants including the exponent n_1 were readily ob-

Table V Kinetic Constants for the Series-Parallel Crystallization Model at 250°C of PPS Doped with Carbon or Graphite Particles

Sample	T_c (°C)	n_1	k_1 (min^{-n_1})	n_2'	k_2' (min^{-n_2})
PPS–carbon[a] (5 wt %)	250	2.5	0.51	1	1.1
PPS–graphite[a] (5 wt %)	250	3.2	5.4	1	2.2

[a] Compounding was done by α-chloronaphthalene solvent.

tained experimentally from the Avrami plots using the early-stage crystallization data. When crystallization entered the second stage after t_d, the kinetic constants for the crystallization of the primary crystal should remain unchanged: the secondary crystal joined in parallel with the primary crystal at this time. The crystallization of the secondary crystal after t_d was a heterogeneous nucleation process with a line growth mechanism ($n_2' = 1$). The value of t_d was taken directly from the location of the discontinuity. The only kinetic constant that had to be estimated from the model was k_2' for the crystallization of the secondary crystal in the later stage.

Similarly, Figure 10 shows that the series-parallel crystallization model describes well the actual crystallization behavior of the graphite-filled PPS (processed with solvent) at 250°C. The kinetic constants for the series-parallel crystallization model are summarized in Table V. All kinetic constants derived for this model are seen to be reasonable, suggesting a physical significance of the model in explaining the crystallization mechanisms of the PPS systems. Figure 10 shows that the straight Avrami equation [eq. (1)] deviates quite significantly from the data in the later stage of crystallization by predicting that X_t approaches the final 100% completion point prematurely. The sequential growth of two types of crystals in the graphite filled-PPS could, on the other hand, be well described by the series-parallel crystallization model.

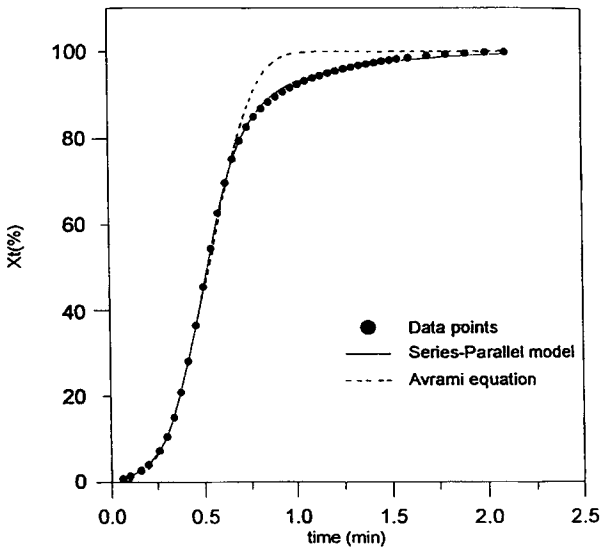

Figure 10 Series-parallel model fitting with the 250°C crystallization data of the graphite-doped PPS samples processed with solvent.

CONCLUSIONS

The crystallization of PPS doped with the carbon or graphite particles has been found to be influenced by the different forms of carbon. Both crystalline graphite and amorphous carbon particles induced a higher crystallization rate of PPS by providing more nucleation sites. In comparison with the neat, unfilled, PPS, the crystallization exponents are lower for the PPS doped with the carbon or graphite particles, suggesting a nucleating effect of the carbon or graphite surface. However, the nucleating effect is different. The crystalline graphite particles have a stronger effect on the overall crystallization rate than did the amorphous carbon. In the Avrami plots, the carbon-filled PPS yielded straight lines while the graphite-filled PPS exhibited an apparent discontinuity at a time corresponding to a separate stage of crystallization taking place. To explain the discontinuity, a series-parallel crystallization model has been proposed to describe the dual crystallization mechanisms of the minor and major crystals. This sequential crystallization model has been shown to describe well the crystallization behavior of PPS systems that exhibit nonlinear Avrami plots.

The financial support (NSC 83-0405-E006-029) provided by National Science Council (NSC) of the Republic of China (Taiwan) is gratefully acknowledged.

REFERENCES

1. T. C. Clarke, K. K. Kanazawa, V. Y. Lee, J. F. Rabolt, J. R. Reynolds, and G. B. Street, *J. Polym. Sci. Polym. Phys. Ed.*, **20,** 117 (1982).
2. P. G. Kelleher, and P. Hubbaur, in *Proceedings of the 36th ANTEC, Society of Plastics Engineers,* 1978, p. 340.
3. J. S. Chung and P. Cebe, *J. Polym. Sci. Polym. Phys. Ed.*, **30,** 163 (1992).
4. G. P. Desio and L. Rebenfeld, *J. Appl. Polym. Sci.*, **44,** 1989 (1992).
5. G. P. Desio and L. Rebenfeld, *J. Appl. Polym. Sci.*, **45,** 2005 (1992).
6. C. Auer, G. Kalinka, TH. Krause, and G. Hinrichsen, *J. Appl. Polym. Sci.*, **51,** 407 (1994).
7. D. R. Budgell and M. Day, *Polym. Eng. Sci.*, **31,** 1271 (1991).
8. A. J. Lovinger, D. D. Davis, and F. J. Padden, Jr., *Polymer,* **26,** 1595 (1986).
9. L. C. Lopez and G. L. Wilkes, *Polymer,* **30,** 882 (1989).
10. L. C. Lopez and G. L. Wilkes, *J. Macromol. Sci. Rev.*, **29,** 83 (1989).
11. I. Koschinski and K.-H. Reichert, *Makromol. Chem. Rapid Commun.*, **9,** 291 (1988).
12. J. Deporter and D. G. Baird, *Polym. Compos.*, **14,** 201 (1993).
13. H. Zeng and G. Ho, *Angew. Makromol. Chem.*, **127,** 103 (1984).
14. J. Karger-Kocsis and K. Friedrich, *J. Mater. Sci.*, **22,** 947 (1987).
15. G. P. Desio and L. Rebenfeld, *J. Appl. Polym. Sci.*, **39,** 825 (1990).
16. J. P. Jog and V. M. Nadkarni, *J. Appl. Polym. Sci.*, **30,** 997 (1985).
17. M. Avrami, *J. Chem. Phys.*, **9,** 177 (1949).
18. U. R. Evans, *Trans. Faraday Soc.*, **257,** 413 (1981).
19. E. M. Woo and J.-M. Chen, *J. Polym. Sci., Polym. Phys. Ed.*, to appear.
20. D. C. Bassett, *Principles of Polymer Morphology,* Cambridge University Press, Cambridge, 1981, Chap. 6.
21. P. Cebe and S. Chung, *Polym. Compos.*, **11,** 265 (1990).
22. P. Huo and P. Cebe, *Colloid Polym. Sci.*, **270,** 840 (1992).
23. S. Z. D. Cheng, Z. Q. Wu, and B. Wunderlich, *Macromolecules,* **20,** 2802 (1987).
24. S. Z. D. Cheng, M.-Y. Cao, and B. Wunderlich, *Macromolecules,* **19,** 1868 (1986).
25. Y. Lee, R. S. Porter, and J. S. Lin, *Macromolecules,* **22,** 1756 (1989).
26. D. J. Blundell, *Polymer,* **28,** 2248 (1987).
27. R. S. Stein and A. Misra, *J. Polym. Sci. Polym. Phys. Ed.*, **18,** 327 (1980).
28. J. T. Yeh and J. J. Runt, *J. Polym. Sci. Polym. Phys. Ed.*, **27,** 1543 (1989).
29. H. J. Ludwig and P. Eyerer, *Polym. Eng. Sci.*, **28,** 143 (1988).
30. H. Marand and A. Prasad, *Macromolecules,* **25,** 1731 (1992).
31. A. J. Lovinger, S. D. Hudson, and D. D. Davies, *Macromolecules,* **25,** 1759 (1992).
32. K. H. Gardner, B. S. Hsiao, and K. L. Faron, *Polymer,* **35,** 2290 (1994).
33. C. Velisaris and J. C. Seferis, *Polym. Eng. Sci.*, **26,** 1574 (1986).
34. P. Cebe, *Polym. Eng. Sci.*, **28,** 1192 (1988).

Received January 3, 1995
Accepted February 5, 1995